A Non-Covalently Bound Redox Indicator for Electrochemical CRISPR-Cas12a and DNase I Biosensors

Tessa Siler,[a†] Logan Stanley,[a†] Mariam Saleem,[b] Artavazd Badalyan*[a,b]

[a]Department of Chemistry and Biochemistry, Utah State University, 0300 Old Main Hill, Logan, UT 84322, USA.

[b]Department of Chemistry, University of Louisiana at Lafayette, 300 East St. Mary Blvd, Lafayette, LA 70504, USA.

[†]Contributed equally.

*Corresponding author: artavazd.badalyan@louisiana.edu.

Abstract

A rapid and accurate biosensor for detecting disease biomarkers at point-of-care is essential for early disease diagnosis and preventing pandemics. CRISPR-Cas12a is a promising recognition element for DNA biosensors due to its programmability, specificity, and deoxyribonuclease activity initiated in the presence of a biomarker. The current electrochemical CRISPR-Cas12a-based biosensors utilize the single-stranded DNA (ssDNA) self-assembled on an electrode surface and covalently modified with the redox indicator, usually methylene blue (MB). In the presence of a biomarker, the nuclease domain is activated and cleaves ssDNA, decreasing the redox indicator signal. The covalent attachment of the MB to the ssDNA implies complexity and a higher production cost. Alternatively, some redox indicators can noncovalently bind to the ssDNA. Although such indicators have been applied for electrochemical nucleic acid detection, their potential for electrochemical CRISPR-Cas-based biosensors has not been explored. In this work, a ruthenium complex, $[Ru(NH_3)_6]^{3+}$, was investigated as a redox indicator non-covalently binding

to the ssDNA. Voltammetric studies and the optimization resulted in a simple and robust electrochemical method that was tested for deoxyribonuclease I (DNase I) activity detection and applied in the CRISPR-Cas12a-based biosensor for viral DNA (HPV-16). The biosensors revealed good analytical properties and represent an alternative to reported biosensors for nuclease activity requiring a covalent attachment of the redox indicator. Moreover, the developed method offers prospects for advancement and can be transformed to operate with other Cas nucleases to detect RNA and other analytes.

Keywords: electrochemical biosensor, nuclease activity, Cas12a, DNase I, redox mediator, voltammetry.

Introduction:

A rapid and accurate biosensor for the detection of disease biomarkers at point-of-care is essential for early disease diagnosis. Electrochemical biosensors for nucleic acid detection have become increasingly important in medical diagnostics, environmental monitoring, and other fields of applications due to their relative simplicity, low cost, fast response, and miniaturization prospects [1,2]. The utilization of CRISPR-Cas (Cluster Regularly Interspaces Short Palindromic Repeats – CRISPR-associated) nucleases in electrochemical biosensors offers promising pathways for nucleic acid detection due to attractive properties of Cas enzymes, such as programmability, high sensitivity, sequence specificity, and others [3–7].

The electrochemical biosensors utilizing CRISPR-Cas nucleases, such as Cas12a, Cas13, and others, have been applied to detect nucleic acids and other classes of analytes. These biosensors employ a signal transduction method based on determining nuclease activity. In electrochemical Cas12a-based biosensors (Figure 1a) [8,9], the Cas12a-nuclease is initially programmed by binding a crRNA, which is designed to recognize target DNA (tarDNA) due to the protospacer adjacent motif (PAM) sequence and the complementary region. When tarDNA is present, its PAM sequence is recognized by the Cas12a-crRNA duplex, followed by unwinding the double-stranded tarDNA. After separating tarDNA strands, Cas12a-crRNA identifies the complementary region of the tarDNA and activates the cis-activity cleaving tarDNA and the trans-nuclease activity. The latter results in non-specific cleavage of numerous ssDNA, also called reporter DNA (repDNA), self-assembled on a gold electrode surface and covalently modified with the redox indicator (Figure 1b). The loss of the redox indicator attached to the electrode surface is proportional to the nuclease activity and determined by an electrochemical technique, square wave voltammetry [10].

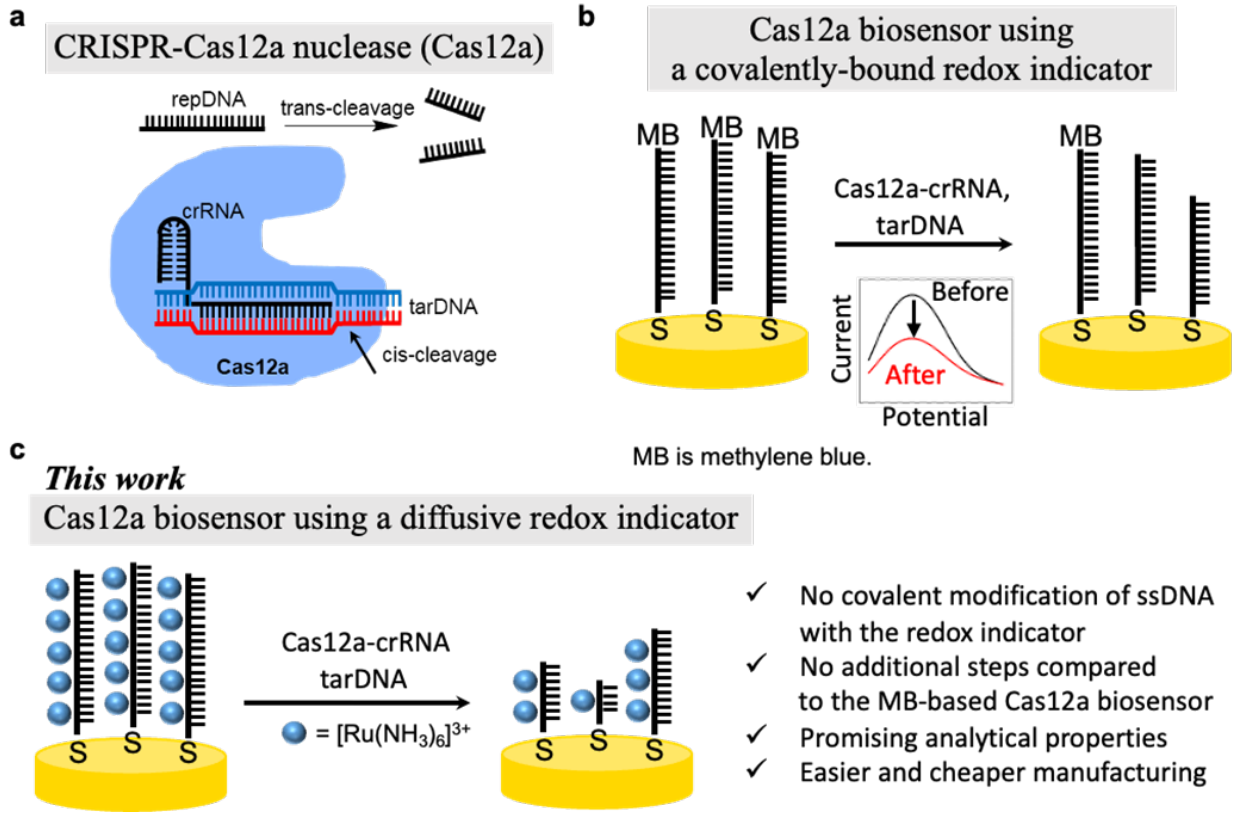

Figure 1. (a) A simplified scheme of CRISPR-Cas12a cis- and trans-nuclease activities. (b) The signal transduction of Cas12a trans-nuclease activity utilizing covalently bound methylene blue (MB) redox reporter. (c) The developed signal transduction scheme for nuclease activity detection based on non-covalently bound redox reporter, $[Ru(NH_3)_6]^{3+}$.

The most widely used redox indicator in electrochemical CRISPR-Cas-based biosensors is methylene blue [9]. The covalent DNA modification with this redox indicator requires additional repDNA synthesis, purification, and characterization steps that introduce complexity in biosensor manufacturing and increase the cost. On the other hand, some redox indicators can non-covalently bind to ssDNA immobilized on the electrode surface [11]. Although such redox indicators have been studied for the on-electrode hybridization biosensors for DNA and RNA detection, their potential for electrochemical CRISPR-Cas-based biosensors has not been explored (Figure 1c). Non-covalently bound redox indicators may significantly simplify the biosensor design, lower costs, and provide alternative detection and signal amplification pathways.

In this work, we studied the properties of a redox indicator, $[Ru(NH_3)_6]^{3+}$, on the electrode modified with a single-stranded DNA, using square wave and cyclic voltammetry. These studies showed approximately 0.12 V difference in the formal potentials for DNA-bound and free ruthenium species, which agrees with previous reports [12–14]. After optimizing the parameters, the electrochemical signal of DNA-bound ruthenium species can be readily distinguished from the free $[Ru(NH_3)_6]^{3+}$. The developed electrochemical approach was applied as an electrochemical signal transduction method for deoxyribonuclease I (DNase I) activity detection and for Cas12a-based biosensor for human papillomavirus 16 (HPV-16).

Results and Discussion

Voltammetric studies of $[Ru(NH_3)_6]^{3+}$ using a ssDNA-modified gold electrode. Square wave voltammetry was applied to study the electrochemical behavior of $[Ru(NH_3)_6]^{3+}$ on a gold electrode modified with MCH. The electrochemical studies were performed in 5 mM Tris buffer, pH 7.4, containing 50 μM $[Ru(NH_3)_6]^{3+}$. The square wave voltammogram revealed a peak at –0.18 V (vs. SCE, Figure 2a, black trace). Similar studies were performed using a ssDNA-modified gold electrode (Figure 2a, red trace). The square wave voltammogram revealed a previously observed signature at -0.18 V (vs. SCE) overlapping with an additional peak at -0.30 V (vs. SCE). The presence of two peaks in square wave voltammograms is similar to the response obtained for this redox indicator on gold electrodes modified with a double-stranded DNA [12].

The cyclic voltammetry studies revealed two redox transitions with formal redox potentials similar to those observed in square wave voltammograms (Figures S1 and S2; see Supporting Information for more details). The peak-to-peak separation and scan rate analysis indicated a different nature of the two redox species. The ruthenium complex signal at -0.18 V (vs. SCE) is

associated with a freely diffusing species. In contrast, the ruthenium species undergoing redox transition at -0.3 V (vs. SCE) represents a metal complex adsorbed on the electrode surface or confined within a thin layer adjacent to the electrode surface. Thus, the redox peak observed in square wave voltammograms at a higher potential was assigned to the free ruthenium species. In contrast, the DNA-bound ruthenium species caused the redox peak at a lower potential, consistent with previous chronocoulometry [15,16] and cyclic voltammetry [13,14] studies.

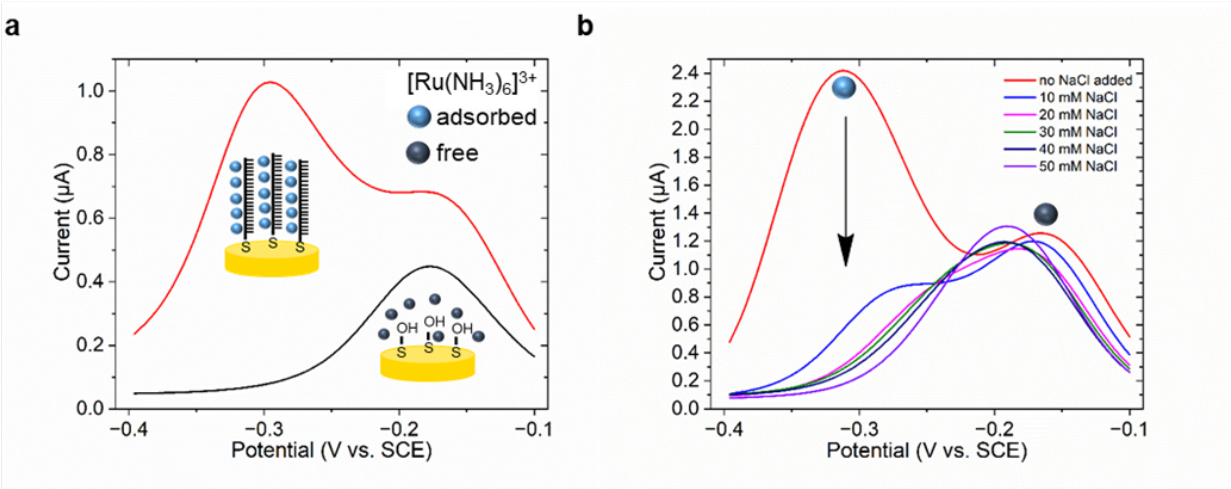

Figure 2. Square wave voltammograms of $[Ru(NH_3)_6]^{3+}$ on chemically modified gold electrodes and the salt effect. (a) Voltammograms were recorded using gold electrodes modified with MCH (black trace) and modified with ssDNA and MCH (red trace) in the presence of 50 μM $[Ru(NH_3)_6]^{3+}$. (b) Voltammograms were recorded using a gold electrode modified with ssDNA and MCH in the presence of 100 μM $[Ru(NH_3)_6]^{3+}$ in 5 mM Tris with no NaCl and after addition of 10 mM, 20 mM, 30 mM, 40 mM, 50 mM NaCl (5 mL).

Optimization of the sensing procedure. To investigate the salt effect, the square wave voltammograms were recorded in 5 mM Tris buffer, pH 7.4, containing 100 μM $[Ru(NH_3)_6]^{3+}$, varying the concentration of NaCl up to 50 mM (Figure 2b). The higher concentration of ruthenium complex was chosen to better follow the signal changes due to the salt effect. The peak associated with adsorbed ruthenium complex was not observed after the addition of 20 mM NaCl, indicating that the electrostatic interactions between positively charged $[Ru(NH_3)_6]^{3+}$ and the negatively

charged phosphate groups on the ssDNA backbone are disrupted by the electrostatic shielding effect. The peak associated with the diffusive $[Ru(NH_3)_6]^{3+}$ showed only minor changes when increasing salt concentration. The electrostatic attraction between the DNA oligomer and metal complex plays a significant role. Further experiments were performed in a 10 mM Tris buffer with no NaCl added.

To find an optimal $[Ru(NH_3)_6]^{3+}$ concentration, the square wave voltammograms were recorded in 10 mM Tris, pH 7.4, varying the concentration of $[Ru(NH_3)_6]^{3+}$ (Figure S3a). At concentrations lower than 10 μM, only the peak of the DNA-bound ruthenium complex was observed and had a relatively low current magnitude. Two peaks were revealed at higher concentrations of $[Ru(NH_3)_6]^{3+}$. The peak current of the adsorbed ruthenium complex peak current increased drastically, more than 20 times, when using 100 μM $[Ru(NH_3)_6]^{3+}$. However, the peak current of the diffusive ruthenium complex was increased as well, which may cause difficulties when detecting low deoxyribonuclease activities.

The final optimization aimed at finding conditions to decrease the current of diffusive ruthenium complex peak and increase the peak current of an adsorbed ruthenium peak. These studies were performed in 50 μM $[Ru(NH_3)_6]^{3+}$, 10 mM Tris, pH 7.4. Inspired by a study [12], the final optimization was achieved by varying the parameters of the square wave voltammetry, such as the pulse amplitude (ΔE), frequency (f), and step potential (E_{st}) (Figure S3b and 3A black trace). This revealed that at higher frequencies, the voltammetric response of the diffusive ruthenium complex is significantly reduced. At the same time, the peak current observed for an adsorbed ruthenium complex increased about ten times was achieved when using a new set of parameters (ΔE = 50 mV, f = 30 Hz, E_{st} = 5 mV).

The developed approach will be used for the electrochemical sensors detecting an ssDNA cleavage activity using square wave voltammetry. It is built upon the understanding provided by the extensive studies performed with various DNA-modified electrodes and ruthenium complex as a redox indicator in the past several decades. Most previous studies were conducted at ruthenium concentrations below 10 μM to suppress the contribution of diffusive redox species (Figure S3a) [13]. Notably, the present work shows that higher concentrations of ruthenium complex can be successfully applied. Our approach results in a higher current response and minimal contribution of a diffusive ruthenium complex, increasing the sensitivity, and may decrease the time required to reach the equilibrium for the adsorption of ruthenium complex onto the DNA backbone, making the method less prone to the time-dependent effects [17].

At higher redox indicator concentrations, the voltammetric procedure is performed in the solution containing redox indicator due to the parameter's optimization and significantly different redox potential of the adsorbed and diffusive species. In contrast, methylene blue applied as a diffusive redox indicator shows no significant potential change. It requires two steps [18]: the incubation in the methylene blue solution and transfer to methylene blue free solution for a voltammetric measurement where the signal is time-dependent due to the diffusion of the redox indicator into the bulk [16,19,20]. Thus, the developed method has essential application advantages beneficial for the detection of deoxyribonuclease activity [16].

Detection of DNase I activity. The developed electrochemical approach was applied first to detect the DNase I activity. The deviation of DNase I activity is an essential marker for clinical and point-of-care diagnostics of several diseases [21]. The lower activity of DNase I results in an increased DNA concentration in the blood, which causes autoimmune diseases [22–24]. The changes in extracellular DNase I activity are essential biomarkers of tumor progression [25].

The square wave voltammograms were recorded for a ssDNA-modified electrode before and after incubating in the solution containing DNase I in the DNase buffer (20 mM Tris buffer pH 7.4, 5 mM $MgCl_2$). The corresponding voltammograms are shown in Figure 3a. More than 90 % of signal loss was observed after incubating an electrode in the solution containing 50 U/mL DNase I. The dependence of the signal loss versus DNase I activity was studied, and a linear behavior between 1 U/mL and 50 U/mL DNase I was revealed (Figure 3b). Interestingly, slightly negative values were observed when no or 0.1 U/mL DNase I was present. This effect may be due to the slight desorption of ssDNA or a very low nuclease activity (0.1 U/mL) that makes the ssDNA layer less dense and more accessible for the ruthenium complex. As a result, more ruthenium species can diffuse inside the DNA layer and bind to the DNA, causing a slight increase in the signal [26].

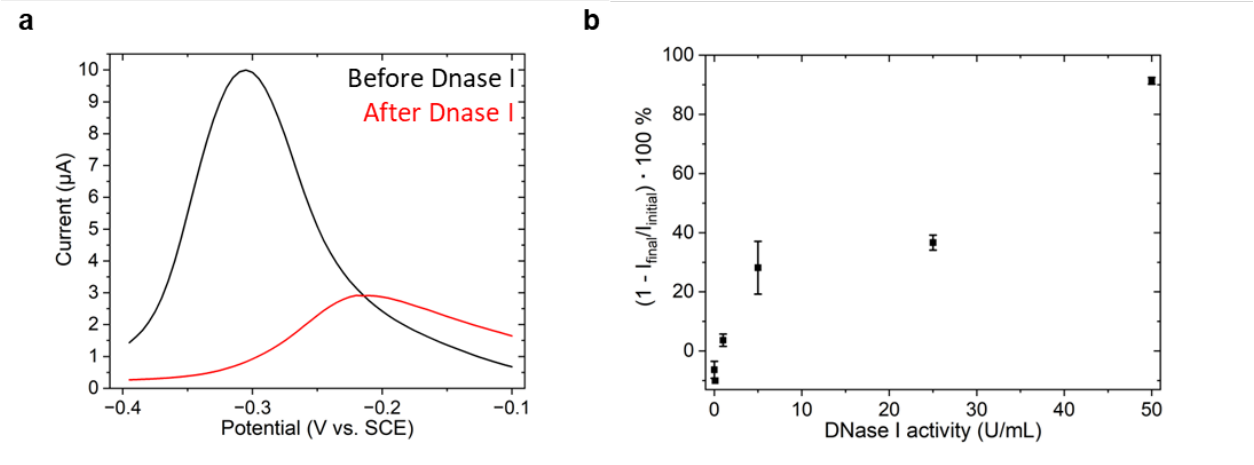

Figure 3. DNase I activity measurements using $[Ru(NH_3)_6]^{3+}$. (a) Voltammograms were recorded using a gold electrode modified with ssDNA and MCH in the presence of 50 μM $[Ru(NH_3)_6]^{3+}$ before and after incubation in the solution containing 50 U/ml DNase I. (b) Loss of the signal of the DNA-bound ruthenium complex versus DNase I activity. Conditions of electrode incubation: 20 mM Tris buffer pH 7.4, 5 mM $MgCl_2$ (n=3). Conditions of electrochemical measurement: 10 mM Tris, pH 7.4 (5 mL).

The linear range of the developed biosensor is similar to published electrochemical biosensors utilizing covalently bound redox indicators (Table S1; see Supporting Information for more details)[27,28]. Thus, the covalent modification of ssDNA can be circumvented when using a

diffusive redox indicator. The ways to advance the analytical characteristics of the developed biosensor are discussed below.

Cas12a biosensor for DNA detection. The potential of the developed electrochemical approach was examined for the Cas12a-based biosensor for HPV-16. The working principle is shown in Figure 1c. The Cas12a-crRNA duplex was prepared by mixing Cas12a and crRNA containing a region to recognize the PAM sequence and a region complementary to the part of the HPV-16 genome (see Supporting Information for more details). The gold electrode modified with ssDNA and MCH was investigated in the presence of ruthenium complex before and after one-hour incubation in the solution containing a Cas12a-crRNA duplex and tarDNA in the "CRISPR buffer" (10 mM Tris pH 7.9, 50 mM NaCl, 15 mM $MgCl_2$, and 100 μg/mL BSA) at 37 ºC.

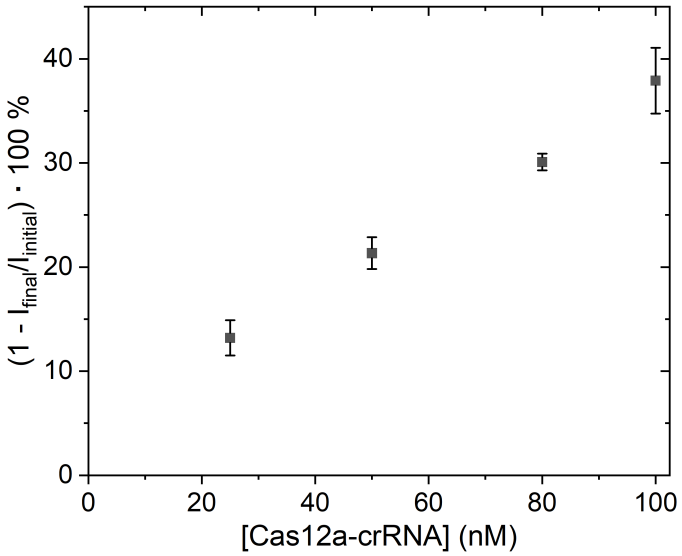

Figure 4. The effect of [Cas12a-crRNA] on the biosensor signal. The dependence of the signal loss as a function of [Cas12a-crRNA]. Conditions of incubation: 260 nM tarDNA, 10 mM Tris pH 7.9, 50 mM NaCl, 15 mM $MgCl_2$, and 100 μg/mL BSA. Conditions of electrochemical measurement: 50 μM $[Ru(NH_3)_6]^{3+}$, 10 mM Tris, pH 7.4.

First, the concentration of Cas12a-crRNA duplex was varied in the presence of the double-stranded tarDNA (Figure 4). The signal loss was observed and increased when higher concentrations of Cas12a-crRNA were used. Then, the Cas12a biosensor signals were studied, varying the concentration of tarDNA in the presence of a 75 nM Cas12a-crRNA duplex (Figure 5a). The response changed significantly below 100 nM tarDNA with the lowest measured concentration of 0.1 nM tarDNA.

To further characterize the biosensor, the relative responses were measured for 260 nM tarDNA and 260 nM single-stranded tarDNA-16 and tarDNA-16c. tarDNA-16c does not contain a PAM sequence, but the complementary regions towards crRNA; tarDNA-16 contains the PAM sequence but no complementary region to crRNA (see Supporting Information for more details). Importantly, the tarDNA concentration was chosen in the saturation range in order not to be limited by the tarDNA. As shown in Figure 5b, the biosensor response is about 1.8 times higher for the tarDNA-16c than for the double-stranded tarDNA. The biosensor response towards the noncomplementary tarDNA-16 is about 5 times lower than for the tarDNA because of the lack of a complementary region, though the PAM sequence is present. Previously[29], the trans nuclease of Cas12a-crRNA was studied with double-stranded tarDNA, single-stranded ssDNA, and a noncomplementary ssDNA after one-hour incubation at 37 ºC using repRNA bearing a fluorophore and a quencher. In the presence of a complementary tarDNA, the repRNA was cleaved and generated a fluorimetric signal. Using ssDNA and dsDNA as targets, similar fluorimetric signals were observed, and very low signals were observed for non-complementary single-stranded tarDNA similar to the developed electrochemical biosensor.

The dynamic range of the developed biosensor is 0.1 nM to 100 nM tarDNA, which is broader than that of the MB-based Cas12a biosensor for HPV-16 (Table S2; see Supporting Information

for more details) [10]. The lowest measured concentrations are similar for the developed and MB-based biosensors. Also, the Cas12a-based biosensors may be affected by the presence of other nucleases and require the separation of nucleic acids from proteins.

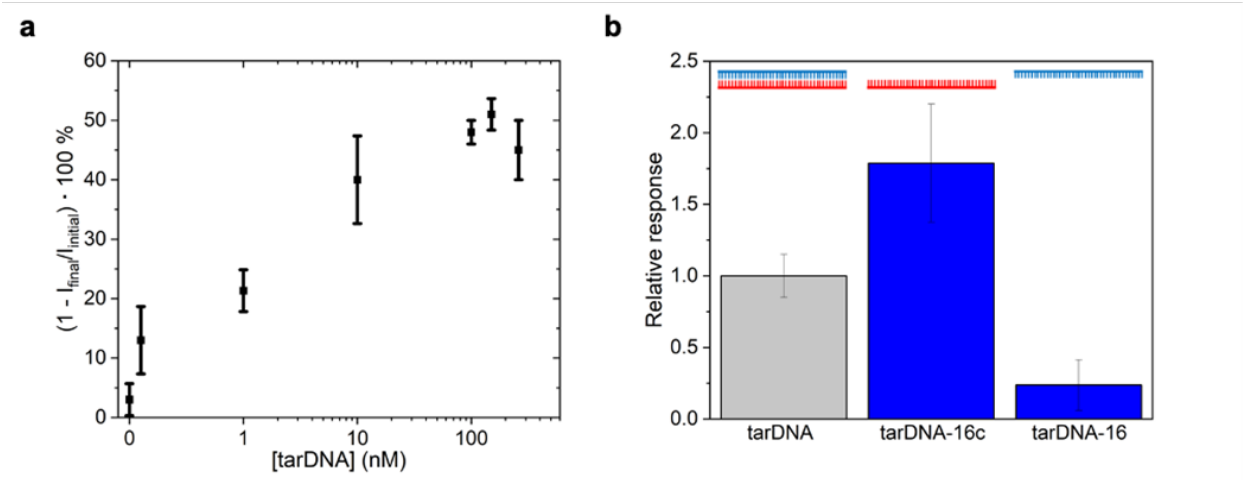

Figure 5. Cas12a biosensor utilizing a diffusive redox indicator. (a) The biosensor signal loss versus [tarDNA]. (b) Relative responses of the Cas12a biosensor towards tarDNA, the complementary ssDNA (tarDNA-16c), and non-complementary ssDNA (tarDNA-16). Conditions of electrode incubation: 75 nM Cas12a-crRNA, 260 nm of tarDNA and other DNAs, 10 mM Tris pH 7.9, 50 mM NaCl, 15 mM $MgCl_2$, and 100 μg/mL BSA (n=3). Conditions of electrochemical measurement: 50 μM $[Ru(NH_3)_6]^{3+}$, 10 mM Tris, pH 7.4 (5 mL).

The developed electrochemical signal transduction method allows the circumventing of the additional covalent modification of the repDNA with a redox indicator for Cas12a biosensors. The sensitivity of the developed biosensors may be significantly advanced by increasing electrode surface area using nanomaterials or electrochemical signal amplification, for example, through electrocatalysis [30]. Moreover, the developed signal transduction system can be used with various CRISPR-Cas nucleases to construct novel biosensors and to study the properties of nucleases.

Conclusions:

Electrochemical CRISPR-Cas-based biosensors for nucleic acids are an emerging technology. Most Cas-based biosensors are based on the nuclease signal transduction, utilizing an ssDNA self-assembled on the gold electrode surface and covalently modified with a redox indicator. This study introduces a new signal transduction method for nuclease and Cas-based biosensors by applying a non-covalently binding redox indicator, a positively charged ruthenium complex. The metal complex electrostatically binds to the ssDNA self-assembled on the gold electrode surface. The optimization of various parameters allowed us to distinguish and evaluate the signal of the DNA-bound ruthenium species, which enabled the detection of deoxyribonuclease activity. The developed approach showed a potential for DNase I and Cas12a-based biosensors and represents a sound alternative to the biosensors utilizing ssDNA covalently modified with a redox indicator, usually methylene blue. This may lead to simpler and lower-cost devices. The developed method can be transformed to operate with other Cas nucleases to detect RNA and other analytes and used to study the properties of various nucleases.

Experimental Section

Reagents. All commercial reagents were obtained from Sigma-Aldrich and used as received unless otherwise noted. Cas12a (Alt-R L.b. Cas12a (Cpf1) Ultra), crRNA, and DNA oligomers were purchased from IDT DNA (see Supporting Information for more details). Dinitrogen was purchased from Air Liquide America Specialty Gases LLC.

Apparatus. Electrochemical measurements were performed on CH Instruments Model 620E (Austin, USA). Voltammograms were measured in an aqueous buffer solution (10 mM Tris, pH 7.4) at room temperature (22-23°C) and purged with N_2 to remove oxygen if not otherwise noted. The conventional three-electrode cell (SVC-2, ALS, Japan) was used with a platinum wire counter

electrode, Saturated Calomel Electrode (SCE, ALS, Japan) as a reference electrode, and a gold (Au) working electrode (diameter 1.6 mm, BASi, USA).

Electrode preparation. Gold electrodes were routinely polished with polishing alumina suspension (1 μm) for 3 minutes, rinsed with water, sonicated for 2 minutes, polished with alumina suspension (0.3 μm), rinsed with water, and sonicated for 10 minutes. After mechanical polishing, the electrodes underwent electrochemical polishing in 0.5 M NaOH between -0.35 V to -1.35 V for 500 scans (scan rate 2 Vs^{-1}) then in 0.5 M H_2SO_4 between -0.3 V to 1.7 V for 10 scans (scan rate 0.3 Vs^{-1}), then in 0.5 M H_2SO_4 with 10 mM NaCl between -0.3 V to 1.7 V for 10 scans (scan rate 0.3 Vs^{-1}), and finally in 0.1 M H_2SO_4 between -0.3 V to 1.7 V for 3 scans (scan rate 0.3 Vs^{-1}) under air.

The ssDNA oligomer modified with the thiol group was deprotected. For this, 5 μL of 200 μM ssDNA oligomer was mixed with 10 μL of 10 mM tris(2-carboxyethyl)phosphine (TCEP) in water for 1 hour at room temperature. Then, 15 μL of reduced ssDNA oligomer were mixed with 1 μL of 1 mM with mercaptohexanol (MCH) and 84 μL of the deposition buffer, containing 50 mM phosphate buffer, 1 M NaCl, pH 7, resulting in the final 10 μM ssDNA and 10 μM MCH. A freshly polished electrode was incubated in this solution overnight at room temperature. The electrode was rinsed with 10 mM Tris, 10 mM NaCl, pH 7.4, passivated in 1 mM MCH for 30 minutes, rinsed again, and used in studies.

Procedures for DNase I and Cas12a biosensors. For the DNase I biosensor, electrodes were incubated for 1 hour at room temperature in 20 mM Tris, 5 mM $MgCl_2$, and pH 7.4, varying concentrations of the DNase I. Then the electrodes were rinsed as described above.

The Cas12a-crRNA duplex was prepared by mixing 1 μl of 67 μM Cas12a and 0.84 μl of 125 μM crRNA for 30 minutes at 37 ºC. Then, the duplex was aliquoted and stored at -20 ºC. For the

Cas12a biosensor, electrodes were incubated for 1 hour at 37 ºC in 10 mM Tris pH 7.9, 50 mM NaCl, 15 mM $MgCl_2$, and 100 µg/mL BSA in the presence of tarDNA if not stated otherwise. Then, the electrodes were rinsed as described above.

ORCID

Artavazd Badalyan: 0000-0002-6933-6181

Author Contributions

A.B. conceived the idea of the project. T.S. and A.B. designed the study. T.S., L.S., and M.S. performed all experimental work and led the data interpretation and analysis in consultation with A.B. A.B. wrote the manuscript.

Notes

The authors declare no competing financial interest.

Associated content

Supporting Information

The supporting information is available free of charge on the ACS Publications website at DOI:

Nucleic acid sequences, cyclic voltammetry studies, and summary of biosensors (PDF).

Acknowledgments

This material is based on work supported by the National Science Foundation under Grant No. 2110313. The authors thank Dr. Lance C. Seefeldt, Dr. Scott Ensign, and Dr. Ryan Jackson for their support and fruitful discussions.

References.

[1] S. Li, H. Zhang, M. Zhu, Z. Kuang, X. Li, F. Xu, S. Miao, Z. Zhang, X. Lou, H. Li, F. Xia, Electrochemical Biosensors for Whole Blood Analysis: Recent Progress, Challenges, and Future Perspectives, Chem. Rev. 123 (2023) 7953–8039.

[2] M. Labib, E.H. Sargent, S.O. Kelley, Electrochemical Methods for the Analysis of Clinically Relevant Biomolecules, Chem. Rev. 116 (2016) 9001–9090.
[3] Y. Yin, J. Wen, M. Wen, X. Fu, G. Ke, X.-B. Zhang, The design strategies for CRISPR-based biosensing: Target recognition, signal conversion, and signal amplification, Biosens. Bioelectron. (2023) 115839.
[4] Y. Li, Y. Liu, X. Tang, J. Qiao, J. Kou, S. Man, L. Zhu, L. Ma, CRISPR/Cas-Powered Amplification-Free Detection of Nucleic Acids: Current State of the Art, Challenges, and Futuristic Perspectives, ACS Sens. 8 (2023) 4420–4441.
[5] M.M. Kaminski, O.O. Abudayyeh, J.S. Gootenberg, F. Zhang, J.J. Collins, CRISPR-based diagnostics, Nat. Biomed. Eng. 5 (2021) 643–656.
[6] J.E. van Dongen, J.T.W. Berendsen, R.D.M. Steenbergen, R.M.F. Wolthuis, J.C.T. Eijkel, L.I. Segerink, Point-of-care CRISPR/Cas nucleic acid detection: Recent advances, challenges and opportunities, Biosens. Bioelectron. 166 (2020) 112445.
[7] Y. Dai, Y. Wu, G. Liu, J.J. Gooding, CRISPR Mediated Biosensing Toward Understanding Cellular Biology and Point-of-Care Diagnosis, Angew. Chem., Int. Ed. 59 (2020) 2–15.
[8] T. Li, N. Cheng, Sensitive and Portable Signal Readout Strategies Boost Point-of-Care CRISPR/Cas12a Biosensors, ACS Sens. 8 (2023) 3988–4007.
[9] C. Yudin Kharismasari, Irkham, M.I.H.L. Zein, A. Hardianto, S. Nur Zakiyyah, A. Umar Ibrahim, M. Ozsoz, Y. Wahyuni Hartati, CRISPR/Cas12-Based Electrochemical Biosensors for Clinical Diagnostic and Food Monitoring, Bioelectrochemistry (2023) 108600.
[10] Y. Dai, R.A. Somoza, L. Wang, J.F. Welter, Y. Li, A.I. Caplan, C.C. Liu, Exploring the Trans-Cleavage Activity of CRISPR-Cas12a (cpf1) for the Development of a Universal Electrochemical Biosensor, Angew. Chem. Int. Ed. 58 (2019) 17399–17405.
[11] E.E. Ferapontova, DNA Electrochemistry and Electrochemical Sensors for Nucleic Acids, Annu. Rev. Anal. Chem. 11 (2018) 197–218.
[12] R. Campos, E.E. Ferapontova, Electrochemistry of weakly adsorbed species: Voltammetric analysis of electron transfer between gold electrodes and Ru hexaamine electrostatically interacting with DNA duplexes, Electrochimica Acta 126 (2014) 151–157. https://doi.org/10.1016/j.electacta.2013.07.083.
[13] H.-Z. Yu, C.-Y. Luo, C.G. Sankar, D. Sen, Voltammetric Procedure for Examining DNA-Modified Surfaces: Quantitation, Cationic Binding Activity, and Electron-Transfer Kinetics, Anal. Chem. 75 (2003) 3902–3907.
[14] E.M. Boon, N.M. Jackson, M.D. Wightman, S.O. Kelley, M.G. Hill, J.K. Barton, Intercalative Stacking: A Critical Feature of DNA Charge-Transport Electrochemistry, J. Phys. Chem. B 107 (2003) 11805–11812.
[15] A.B. Steel, T.M. Herne, M.J. Tarlov, Electrostatic Interactions of Redox Cations with Surface-Immobilized and Solution DNA, Bioconjugate Chem. 10 (1999) 419–423.
[16] A. Abi, A. Safavi, Determination of the binding site size of hexaammineruthenium(III) inside monolayers of DNA on gold, Analyst 146 (2021) 547–557.
[17] R. Lao, S. Song, H. Wu, L. Wang, Z. Zhang, L. He, C. Fan, Electrochemical Interrogation of DNA Monolayers on Gold Surfaces, Anal. Chem. 77 (2005) 6475–6480.
[18] C. Li, X. Chen, N. Wang, B. Zhang, An ultrasensitive and label-free electrochemical DNA biosensor for detection of DNase I activity, RSC Adv. 7 (2017) 21666–21670.
[19] A. Erdem, K. Kerman, B. Meric, M. Ozsoz, Methylene Blue as a Novel Electrochemical Hybridization Indicator, Electroanalysis 13 (2001) 219–223.

[20] K. Kerman, D. Ozkan, P. Kara, B. Meric, J.J. Gooding, M. Ozsoz, Voltammetric determination of DNA hybridization using methylene blue and self-assembled alkanethiol monolayer on gold electrodes, Analytica Chimica Acta 462 (2002) 39–47.
[21] S. Sato, S. Takenaka, Highly Sensitive Nuclease Assays Based on Chemically Modified DNA or RNA, Sensors 14 (2014) 12437–12450.
[22] M. Napirei, S. Wulf, H.G. Mannherz, Chromatin breakdown during necrosis by serum Dnase1 and the plasminogen system, Arthritis & Rheumatism 50 (2004) 1873–1883.
[23] M.J. Walport, Lupus, DNase and defective disposal of cellular debris, Nat Genet 25 (2000) 135–136.
[24] S. Tsukumo, K. Yasutomo, DNaseI in pathogenesis of systemic lupus erythematosus, Clinical Immunology 113 (2004) 14–18.
[25] L. Alekseeva, N. Mironova, Role of Cell-Free DNA and Deoxyribonucleases in Tumor Progression, International Journal of Molecular Sciences 22 (2021) 12246.
[26] M. Grubb, H. Wackerbarth, J. Wengel, J. Ulstrup, Direct Imaging of Hexaamine-Ruthenium(III) in Domain Boundaries in Monolayers of Single-Stranded DNA, Langmuir 23 (2007) 1410–1413.
[27] S. Sato, K. Fujita, M. Kanazawa, K. Mukumoto, K. Ohtsuka, S. Takenaka, Reliable ferrocenyloligonucleotide-immobilized electrodes and their application to electrochemical DNase I assay, Anal. Chim. Acta. 645 (2009) 30–35.
[28] S. Sato, K. Fujita, M. Kanazawa, K. Mukumoto, K. Ohtsuka, M. Waki, S. Takenaka, Electrochemical assay for deoxyribonuclease I activity, Anal. Biochem. 381 (2008) 233–239.
[29] J.S. Chen, E. Ma, L.B. Harrington, M.D. Costa, X. Tian, J.M. Palefsky, J.A. Doudna, CRISPR-Cas12a target binding unleashes indiscriminate single-stranded DNase activity, Science 360 (2018) 436–439.
[30] M.A. Lapierre-Devlin, C.L. Asher, B.J. Taft, R. Gasparac, M.A. Roberts, S.O. Kelley, Amplified Electrocatalysis at DNA-Modified Nanowires, Nano Lett. 5 (2005) 1051–1055.

TOC graph

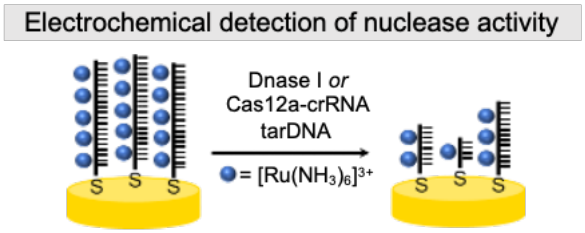

- ✓ No covalent modification with redox indicator
- ✓ Promising analytical properties
- ✓ Simpler and lower cost manufacturing